Robust PU foam skeleton coated with hydroxylated BN as PVA thermal conductivity filler via microwave-assisted curing

Wenbo Wang[1], Botao Liu[1], and Xiaomeng Lv[1,*] ⓘD

[1] *School of Chemistry and Chemical Engineering, Jiangsu University, Zhenjiang 212013, People's Republic of China*

ABSTRACT

To achieve adaptation to the heat dissipation effect of electronic devices in the 5G era and improvement of the anisotropic thermal conductivity of the insulating polymer, three-dimensional (3D) PU@BNNS-OH network structure was constructed via layer-by-layer assembly with polyurethane (PU) foam as the robust skeleton of three-dimensional structure, and hydroxylated boron nitride nanosheet (BNNS-OH) as thermal conductive filler. Then PU@BNNS-OH was composited with polyvinyl alcohol (PVA) via microwave-assisted curing method to get the final thermal conductivity composites (PVA/PU@BNNS-OH). The result showed that the interconnected thermal conductivity network was significantly effective in improving the anisotropic thermal conductivity of the composite with high-temperature endurance and moderate mechanical property. When the BNNS-OH coating is 10 wt%, the optimal thermal conductivity of the composite is 4.68 W· m^{-1}· K^{-1} and the thermal conductivity enhancement efficiency is 45.50, which is significantly higher than others reported in the literature. Both the finite element analysis and thermal infrared analysis indicated that the thermal conductivity of the composites was significantly improved and paved the way for its potential application. The present microwave-assisted synthesis strategy is fast and energy-saving and can be widely used for synthesizing different insulated polymer-based thermal interface materials.

Wenbo Wang and Botao Liu have contributed equally to this paper.

Address correspondence to E-mail: laiyangmeng@163.com

1 Introduction

With the thinning, multi-functionality, and high power of advanced microelectronic devices development, a large amount of heat accumulation causes serious problems, especially in the era of 5G communication ages [1–3]. Effective heat dissipation has become an urgent necessity in many areas, such as electrical insulation, packaging materials, plastic, aerospace, and other related fields [4–6]. The ideal thermal conductive material should have good processing properties, low coefficient of thermal expansion, and good mechanical properties. Recently, polymer materials have received widespread attention due to their superior performance to meet current thermal management needs. However, the low intrinsic thermal conductivity of most polymers has limited their wide application [7, 8]. Recently, there has been a lot of research to add thermally conductive filler to the polymer to increase the thermal conductivity of the polymer [9–11]. The filler with high thermal conductivity is a crucial factor to enhance the thermal conductivity of polymers. Many types of fillers, such as Ag [6], Carbon nanotubes [12], Al_2O_3 [13], SiC [14], nano diamond [15, 16], graphene/graphene oxide [17, 18], and TiO_2 [19], have been investigated. Among them, two-dimensional layered materials such as BN [6, 20, 21] have received extensive attention due to their high thermal conductivity, electrically insulating, and easy operation. In addition to different types of fillers, there are still several issues worth considering as to prepare the polymer-based composite thermal conductivity materials.

Filler loading in the polymer is a key factor affecting thermal conductivity and mechanical properties of the composite. Since the thermal conductivity cannot be increased at the expense of the processing properties and mechanical properties of the composite, a suitable ratio of filler to polymer should be considered. The distribution and orientation of the filler in the polymer also has a great impact on the thermal conductivity. A vertically aligned array of thermally conductive networks is ideal to be built into the polymer. In order to improve the distribution and orientation of the filler in the polymer, hot pressing [22, 23], electro-spinning [24, 25], magnetic alignment [26, 27], vacuum-assisted infiltration [28], and flow-induced orientation [29] are utilized.

However, most methods can only improve the thermal conductivity of a two-dimensional material in a certain direction, and it is hard to simultaneously increase the thermal conductivity of the composite on the in-plane and through-plane. Construction of 3D thermal network is a promising way to solve this problem [11]. Wong et al. synthesized interconnected and vertically aligned graphene network working as effective thermally conductive fillers, with ultralow loading of graphene but extraordinary thermal conductivity of the composite [30]. Further work was focused on constructing 3D BN nanosheets as thermal transfer network and then infiltrated with epoxy matrix as useful thermal interface materials [31]. Hence, the constructing of 3D network can fulfill the low loading of filler with high thermal conductivity, yet its scalable application was still hampered by its complicated synthesis methology, such as ice-templating, chemical vapor deposition, which was always time-consuming and complex processing.

Recently, the utilization of functionalized commercial sponge, due to its low density, porous structure, tractable property, has been considered as ideal substrates in the field of oil–water separation [32], flexible electrode [33], etc., has aroused great interest. As interconnected thermal transfer substrate, functionalized sponge has made a breakthrough in the field of thermal interface materials. Wu et al. used 3D melamine sponge as substrate and supported BN as thermal conductivity filler. The obtained 3D materials were further encapsulated with epoxy to achieve enhanced thermal conductivity at low loading of filler with the method of layer-by-layer assembly [34]. To achieve efficient contact between substrate and filler, and filler and polymer, more favorable combination method needs investigation. In the present work, we used PU foam as a three-dimensional network, and BNNSs were tightly grown on the PU foam substrate by layer-by-layer assembly. Then, a dense layer of PVA film was closely coated on the surface of PU@BNNS-OH by a microwave-assisted curing method to avoid the poor interface contact. The results showed that the three-dimensional thermal transfer network was beneficial to the thermal conductivity of the composite. The optimal BN loading amount was determined via measuring the thermal conductivity. Meanwhile, finite element analysis (FEA) and thermal infrared analysis were carried out to test the heat dissipation

performance using the composite as a heat sink for electronic devices.

2 Experimental

2.1 Materials

Hexagonal boron nitride powder (99.9%, 100 nm) and Polyethyleneimine (PEI, 99%, MW = 10,000) were purchased from Aladdin Reagent (Shanghai) Co., Ltd. Isopropanol (AR), PVA (99%, 1750 ± 50) and Lithium chloride (LiCl·2H$_2$O, 99.9%) were purchased from Sinopharm Chemical Reagent Co., Ltd. Polyurethane foam was purchased from Ligu International Trading (Shanghai) Co., Ltd.

2.2 Exfoliation and hydroxylation of BN

0.25 g of commercial BN powder was dissolved in 50 mL isopropanol solution, and ultrasonically exfoliated for 1 h to obtain BN/isopropanol mixed solution. After exfoliating, BN block was removed by centrifugation, and a uniform and stable BN dispersion was obtained. The BN dispersion was placed in a Teflon reactor for hydrothermal treatment under 160 °C for 8 h to obtain hydroxylated boron nitride nanosheets (BNNS-OH). In order to increase the yield of BNNSs, a small amount of LiCl·2H$_2$O was added into the Teflon reactor [35]. After hydrothermal synthesis, the mixture was washed and centrifugated at 8000 r/min for 5 min and 2000 r/min for 10 min, respectively to get final powder.

2.3 Preparation of PU@BNNS–OH foam

The PU foam (6 cm × 1.5 cm × 0.5 cm) was cleaned and soaked in the PEI (1 mg mL^{-1}) aqueous solution for activation, then washed 2–3 times with deionized water, and then immersed in the BNNSs solution. BNNSs were tightly coated on the PU foam skeleton due to the electrostatic interaction between the activated PU foam and BNNS-OH. This step was repeated iteratively, and the PU/BNNS-OH foam was prepared by layer-by-layer (L-B-L) assembly deposition cycle. We repeated deposition 30 times in this experiment.

2.4 Preparation of PVA/PU@BNNSs composite

We used a microwave reactor (XH-MC-1, 300 W) to deposit a dense film on the surface of the foam at a power of 300 W and a heating time of 120 s. Since the wave absorption performance of the PU foam is significantly better than that of the polymer, the PU/BNNS-OH foam after absorbing microwave was evenly heated, causing the adsorbed PVA solution to rapidly solidify on both the inner and outer surface of porous 3D materials. Hence, a dense layer of PVA film will be formed on the surface of the PU foam, and the PU@BNNS-OH can be actively combined with the PVA to obtain the closely integrated composite. Compared with the vacuum-assisted filtration method and the vacuum-assisted drying method, the microwave-assisted method can greatly shorten the synthesis time and obtain a tight and evenly distributed surface. According to the mass ratio of BNNS-OH to PVA, we labeled the prepared materials as PVA/PU@BNNS-OH-X wt%. Detailed synthesis procedure was illustrated in Fig. 1.

2.5 Characterization

The morphology of the BNNSs, PU foam, PU/BNNSs foam, and PVA/PU@BNNSs composite were characterized by scanning electron microscopy (SEM) (JEOL, JSM-7800F, Japan). A D8 advance X-Ray
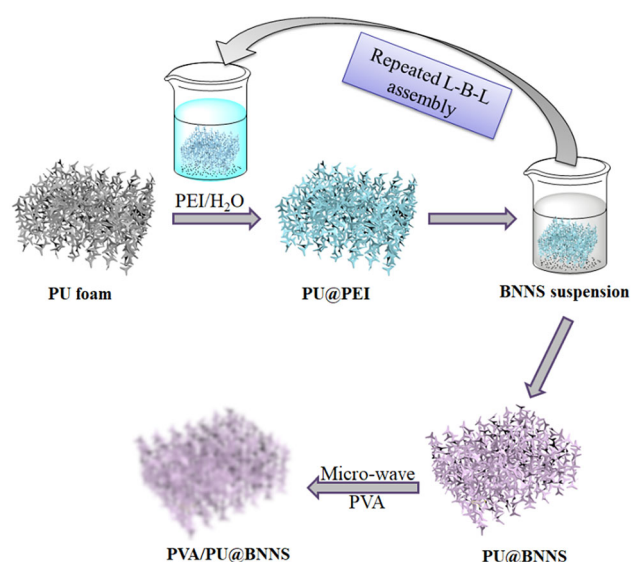

Fig. 1 Preparation process of PU@BNNS-OH foam and PVA/PU@BNNS-OH composite

Diffractometer (XRD) (Bruker, Germany) was used to measure the XRD patterns. Thermogravimetric analysis was carried out at a heating rate of 10 °C min^{-1} under N$_2$ atmosphere using a comprehensive thermal analyzer (Netzsch STA449F3). Thermal conductivity of the samples was directly measured by thermal conductivity measuring instrument (Sweden, Hot Disk, TPS 2500S) using the Transient Plane Source Method (TPS). The composite was cut into 1 × 6 cm strips, and the stress–strain curve of the material was obtained using a universal material testing machine (TH-8201S) at a temperature of 18 °C and a humidity of 56.2%. The thermal radiation effect of the composite on the surface of the LED lamp was observed by a thermal infrared imager (Thermovision A40).

3 Results and discussion

3.1 Functional grouping and hydrogen bonding

Improving the interfacial contact between the filler and the polymer substrate helps to reduce the interfacial thermal resistance. Therefore, we used isopropyl alcohol to realize BNNS surface hydroxylation and prepared BNNS-OH by hydrothermal stripping. The hydroxylated BNNS facilitate intact contact with PVA via the hydrogen bonding of surface functional group.

Figure 2a shows the XRD pattern of commercial h-BN powder and BNNS-OH. The characteristic diffraction peak at 26.76°, 50.10°, 59.56°, and 75.9° can be readily indexed to (002), (100), (004), and (110)

planes of h-BN (JCPDS 34-0421), respectively [36]. The peak position of BNNSs after hydrothermal stripping is almost identical to that of the original commercial h-BN powder, indicating that the hexagonal lattice is not damaged during the stripping process. Taking the (002) peak as a reference, the relative intensity of the (100), (004) and (110) diffraction peaks of BNNS is significantly lower than that of the h-BN powder. This may be due to the enhanced exposure of the (002) plane, since several layers of BNNS tend to be stripped along the (002) plane [8]. Therefore, there is sufficient evidence to prove that the preparation of BNNS-OH is successful. Besides, PU@BNNS-OH foam is rich with a large amount of hydroxyl groups, and PVA is full of plenty of hydroxyl groups, so hydrogen bonds are easily formed between them. Therefore, when PVA and PU@BNNS-OH are cured under microwave irradiation, they would be tightly joined by hydrogen bonding as shown in Fig. 2b [37].

3.2 Morphology and structure

The morphology of the original PU foam and final product was characterized by SEM. Figure 3a shows the original PU foam that displays 3D interconnect macroporous structure with a smooth surface. Figure 3b–d shows the morphology of different BNNS-OH loading combining with PVA, and the foam-supported 3D network still exists clearly. Figure 3b shows the morphology of PVA/PU@BNNS-OH-3 wt%. BNNS-OH is scattered on the foam, and when the BNNS-OH loading is 10 wt%, BNNS-OH is
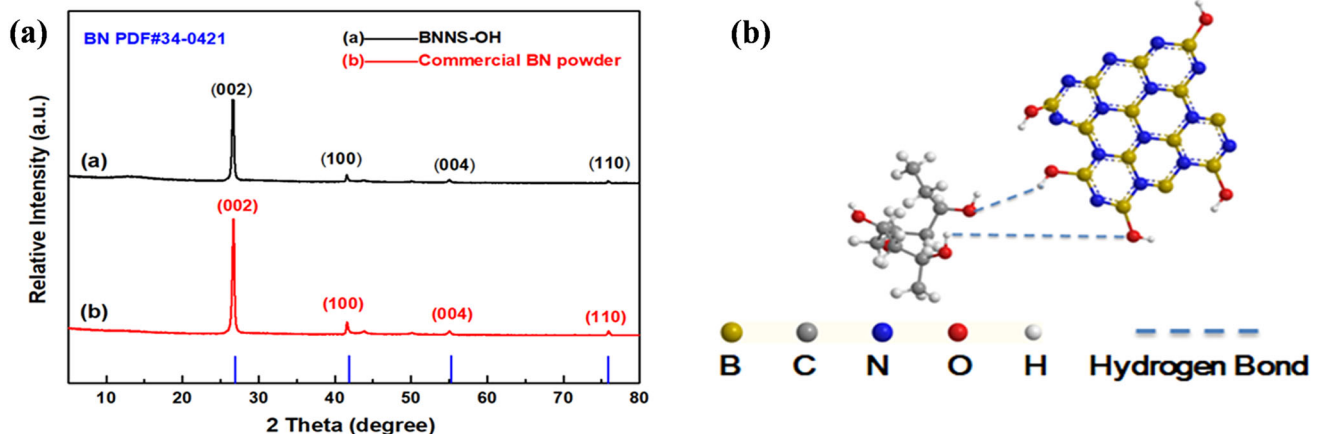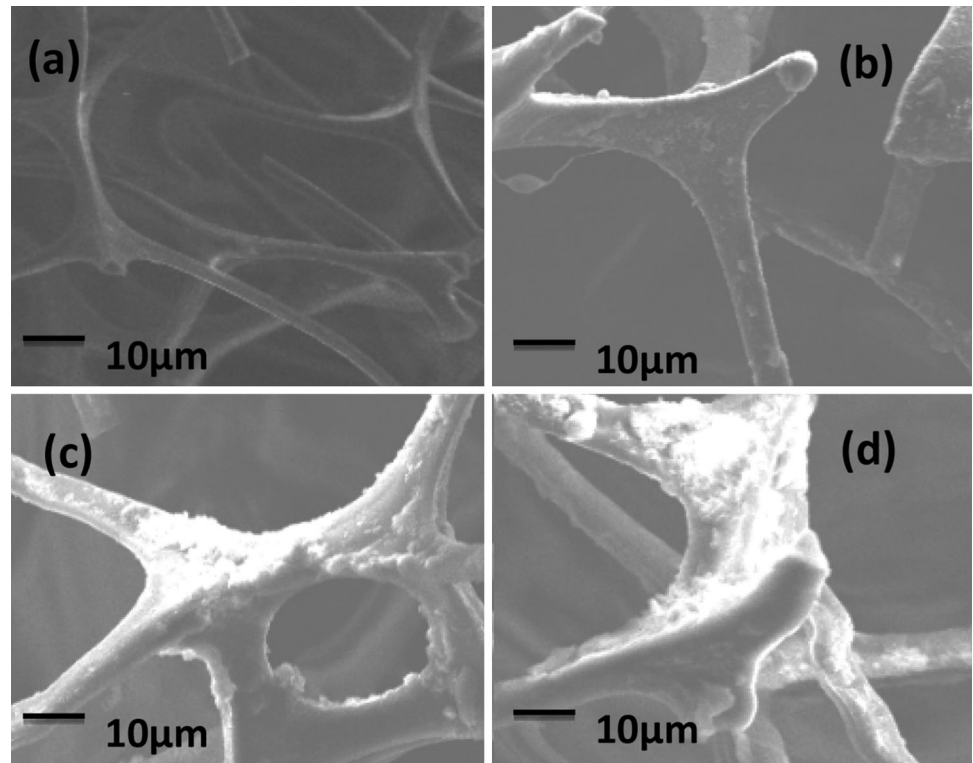

Fig. 2 a XRD patterns of commercial BN powder and BNNS-OH. b Schematic diagram of intermolecular hydrogen bonding between PVA and PU@BNNS-OH

Fig. 3 SEM image of **a** PU foam, **b** PVA/PU@BNNS-OH-3wt%, **c** PVA/PU@BNNS-OH-10wt%, **d** PVA/PU@BNNS-OH-15wt%

evenly distributed on the foam with the 3D interconnected network maintained throughout the PVA matrix, forming heat transfer highway (Fig. 3c). When BNNS-OH loading continues to increase to 15%, excess BNNS-OH will accumulate on the surface of the foam, which will cause local heat concentrated and adversely affect the interface thermal conductivity of composite as in Fig. 3d.
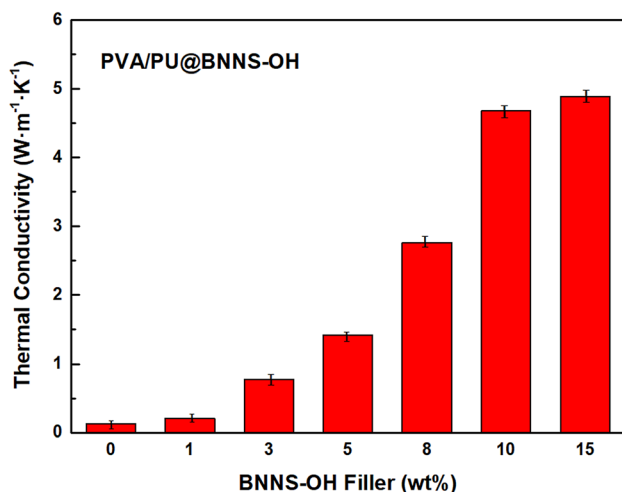

Fig. 4 Thermal conductivity of PVA/PU@BNNS-OH with different BNNS-OH loading

3.3 Thermal conductivity

The thermal conductivity of the prepared PVA/PU@BNNS-OH was measured at room temperature. Meanwhile, the thermal conductivity of the pure PVA film was also measured as a comparison.

Figure 4 shows that the thermal conductivity of the pure PVA film is 0.13 W· m^{-1}· K^{-1}. The thermal conductivity of the composites gradually increases as the BNNS-OH loading increased. When the BNNS-OH loading is 10 wt%, the thermal conductivity is 4.68 W· m^{-1}· K^{-1}. To compare the previous research about thermal conductivity of polymer/BN composites, the thermal conductivity enhancement efficiency (η) is introduced, which is the enhancement of thermal conductivity (ΔTC) divided by the amount of BN loading (L), expressed as follows:

$$\eta = \frac{\Delta TC}{L} = \frac{TC - TC_0}{L}$$

where TC and TC_0 represent the thermal conductivity of the prepared composite and the thermal conductivity of the pure polymer substrate, respectively. L represents the percentage of addition of BN.

After calculation, the maximum value of η is 45.5, which is not result of composit with 15 wt% BN loading but 10 wt% BN loading, suggesting excess

Table 1 Previous studies using BN as a thermally conductive filler

Sample	Filler loading (wt%)	Polymer TC_0 (W·m^{-1}·K^{-1})	Sample TC (W·m^{-1}·K^{-1})	η	Ref
Epoxy/BNNS	16.9	0.18	3.13	17.46	[34]
PDMS/BNNS + GO foam	33.8	0.18	2.11	5.71	[38]
Epoxy resin/BNNS	40	0.4	6.00	14.00	[39]
BN nanoplatelet/PVA	10	0.13	0.34	2.10	[40]
Epoxy/BNNS	16.4	0.18	2.8	15.97	[41]
PVA/PU@BNNS-OH	10	0.13	4.68	45.5	This work

BNNS-OH buildup with 15 wt% loading leading to a decrease in the η value. Here, we summarize previous studies using BN as a thermally conductive filler and calculate their η values, as shown in Table 1.

Obviously, our η value is significantly higher than the previous report with moderate BN loading. Furthermore, we also prepared PVA/BNNS-OH composites under the same loading conditions and compared their thermal conductivity with that of PVA/PU@BNNS-OH. From Figs. 4 and 5a, we can clearly see that the composite containing the 3D structure of the PU foam as support has a higher thermal conductivity than the conventional PVA/BNNS-OH composite, further demonstrating that the 3D structure of the PU foam is helpful for heat conduction. Therefore, we present a promising heat transfer model. Figure 5b shows that when heat propagates through the composite from left to right, heat can be conducted from multiple directions due to the presence of 3D structure, which greatly speeds up the heat dissipation.

3.4 Mechanical properties and thermal stability

The mechanical properties of composite materials are critical to the application of thermal management. We selected the PVA/PU@BNNS-OH film with the largest η value for the stress–strain test. Figure 6a indicates that the tensile strength of PVA/PU@BNNS-OH is up to 87.05 MPa, and the Young's modulus is up to 1200.69 MPa. Due to the presence of PU@BNNS-OH, the mechanical properties of the composite film are inevitably slightly lower than the pure PVA film. Since the fillers enhance thermal conductivity while damaging the mechanical properties of the composite, it is still a challenge to significantly increase the thermal conductivity of the composite under lower filler loading conditions to
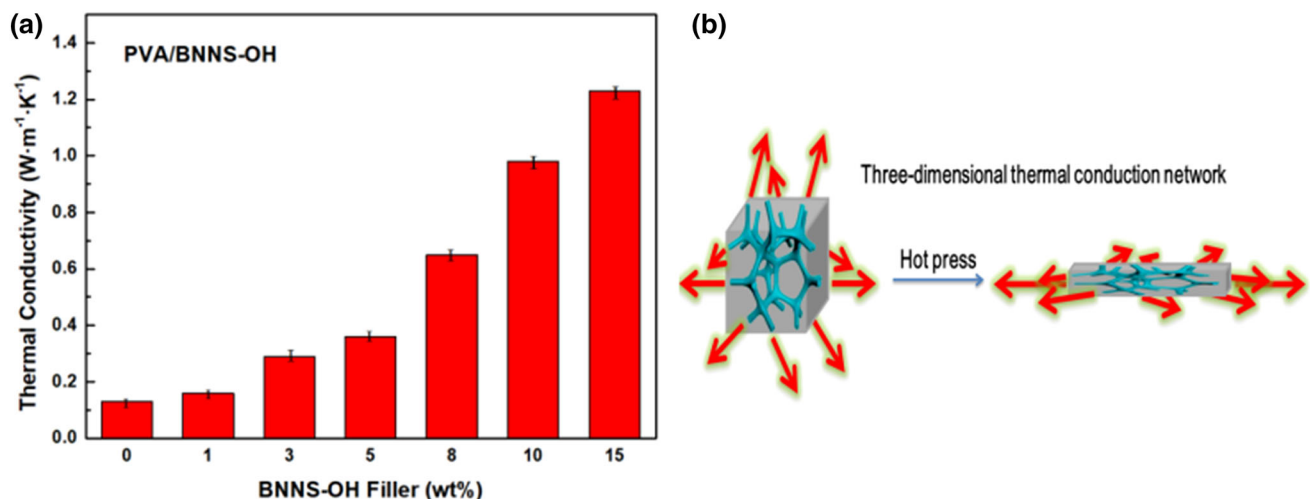

Fig. 5 a Thermal conductivity of PVA/BNNS-OH composites without PU foam supported. **b** Proposed model of PVA/PU@BNNS-OH for thermal conduction
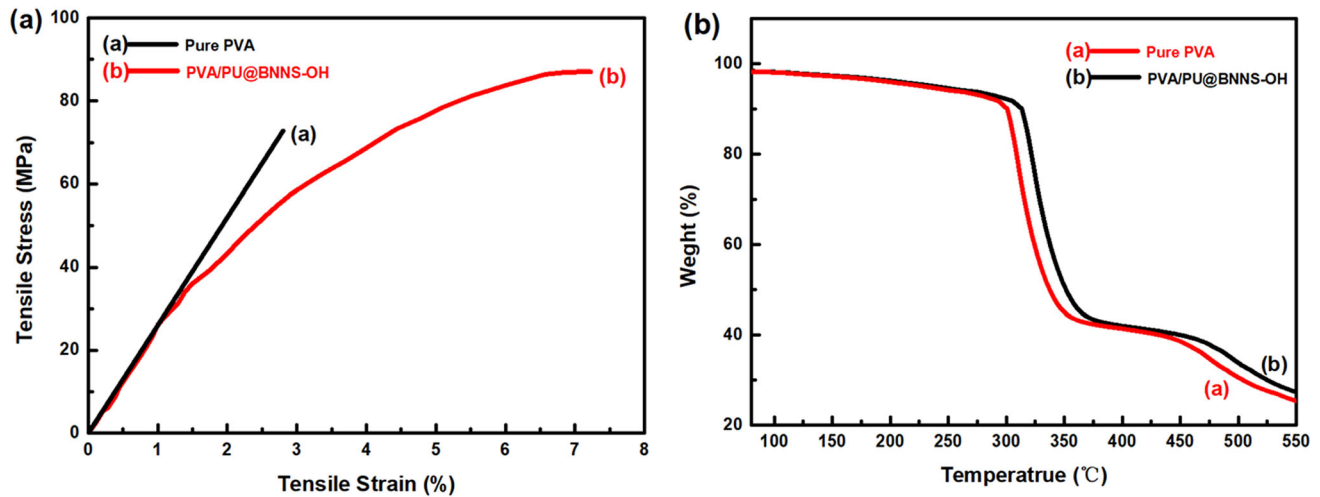
Fig. 6 a Stress–strain curves of pure PVA and PVA/PU@BNNS-OH-10wt%. **b** TGA curves of pure PVA and PVA/PU@BNNS-OH-10wt%

reduce damage to the mechanical properties of the composite.

Good high-temperature resistance is essential for thermal conductive materials application. Figure 6b shows that PVA/PU@BNNS-OH maintains small weight loss till 325 °C. The heat endurance of the composite is slightly higher than that of pure PVA due to the existence of PU@BNNS-OH, facilitating its application under harsh conditions.

3.5 Heat transfer test

The radiator model of Finite element analysis (FEA) was applied to explore the good heat dissipation performance using the composite as a heat sink for electronic devices. Figure 7 shows a radiator with four fins distributed in the vertical direction. The base is a heat source with a power of 3 W LED chip. Figure 7a is a heat transfer diagram of a composite with a thermal conductivity of 4.68 W· m^{-1}· K^{-1}. Figure 7b is a heat transfer diagram without the addition of a thermally conductive composite. It can be seen from the finite element analysis that the overall
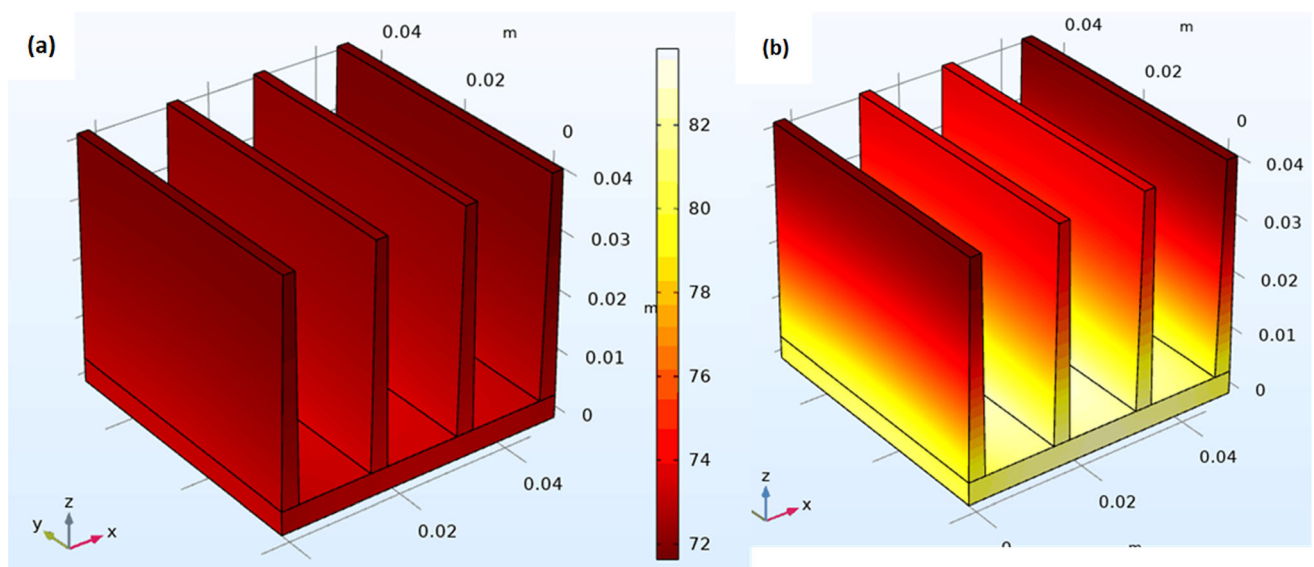

Fig. 7 a Heat transfer simulation of LED chip with thermal composite. **b** Heat transfer simulation of LED chip without thermal composite
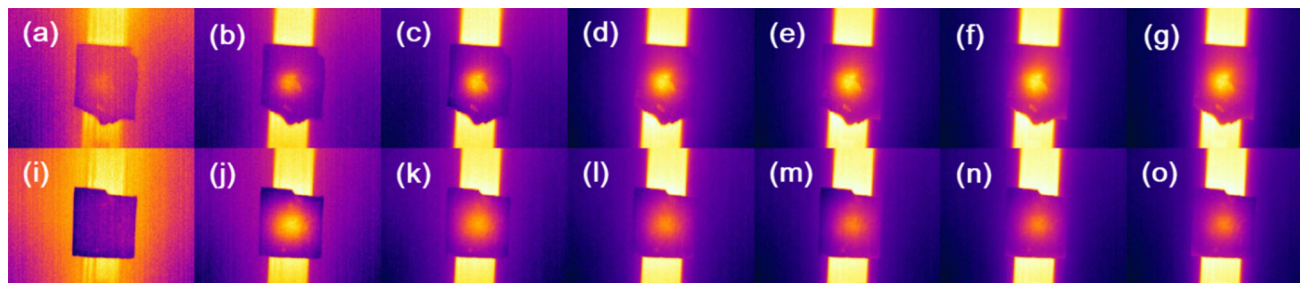
Fig. 8 **a**–**g** are pictures of the PVA/PU in thermal infrared imaging at 0 s, 10 s, 20 s, 30 s, 40 s, 50 s, 60 s. **i**–**o** are pictures of the PVA/PU@BNNS-OH in thermal infrared imaging at 0 s, 10 s, 20 s, 30 s, 40 s, 50 s, 60 s

temperature of Fig. 7a is lower, about 72–74 °C, while the temperature of Fig. 7b is distributed at 72–82 °C. Obviously, it can be seen that the heat dissipation effect of Fig. 7a is better due to the presence of the heat conductive material. This also pays the way for further application of the composite.

In order to further demonstrate the practical application of the composite, we placed PVA/PU@BNNS-OH and PVA/PU on the LED lamp at the same time, and used the thermal infrared analyzer to detect the temperature change of the composite surface at different time interval (0–60 s). Obviously, the sample without BNNS-OH showed a higher centered temperature with more distinguished bright zone as shown in Fig. 8a–g, while the PVA/PU@BNNS-OH exhibited better heat radiation with faint light, as shown in Fig. 8i–o.

4 Conclusion

In summary, we use PU foam as the skeleton of the three-dimensional thermal network, and form 3D thermal conductive filler by loading BNNS-OH, and then prepare PVA/PU@BNNS-OH composite by microwave-assisted method. Due to the existence of the three-dimensional network, the thermal conductivity of the material is greatly improved. The thermal conductivity is 4.68 W$\cdot$ m$^{-1}\cdot$ K^{-1} with 10wt% BNNS-OH loading, and thermal conductivity enhancement efficiency (η) is 45.5. In addition, the tensile strength of PVA/PU@BNNS-OH is up to 87.05 MPa, the Young's modulus is up to 1200.69 MPa, and the degradation temperature is up to 325 °C, suggesting excellent mechanical properties and high-temperature resistance. Finite element analysis and thermal infrared imaging both indicate the heat dissipation effect of the ternary composite is better than binary composite under same condition. Hence, PVA/

PU@BNNS-OH has potential application in high performance thermal management devices during the 5G era due to these brilliant properties.

Declarations

Conflict of interest The authors declare that they have no conflict of interest.

References

1. F. Jiang, N. Song, R. Ouyang, P. Ding, Wall density-controlled thermal conductive and mechanical properties of three-dimensional vertically aligned boron nitride network-based polymeric composites. ACS Appl. Mater. Inter. **13**, 7556–7566 (2021)
2. F. Jiang, S. Zhou, T. Xu, N. Song, P. Ding, Enhanced thermal conductive and mechanical properties of thermoresponsive polymeric composites: Influence of 3D interconnected boron nitride network supported by polyurethane@polydopamine skeleton. Compos. Sci. Technol. **208**, 10877 (2021)
3. X. Bai, C. Zhang, X. Zeng, L. Ren, R. Sun, J. Xu, Recent progress in thermally conductive polymer/boron nitride composites by constructing three-dimensional networks. Compos. Commun **24**, 100650 (2021)

4. Y. Zhang, Y. Liu, Y. Cao, L. Cao, X. Zheng, J. Wang, Y. Pan, N. Wang, Effect of well-designed graphene heat conductive channel on the thermal conductivity of C/SiC composites. Ceram. Int. **47**, 19115–19122 (2021)

5. Q. Yan, W. Dai, J. Gao, X. Tan, L. Lv, J. Ying, X. Lu, J. Lu, Y. Yao, Q. Wei, R. Sun, J. Yu, N. Jiang, D. Chen, C.P. Wong, R. Xiang, S. Maruyama, C.T. Lin, Ultrahigh-aspect-ratio boron nitride nanosheets leading to superhigh in-plane thermal conductivity of foldable heat spreader. ACS Nano **15**, 6489–6498 (2021)

6. C. Chen, Y. Xue, Z. Li, Y.F. Wen, X.W. Li, F. Wu, X.J. Li, D. Shi, Z.G. Xue, X.L. Xie, Construction of 3D boron nitride nanosheets/silver networks in epoxy-based composites with high thermal conductivity via in-situ sintering of silver nanoparticles. Chem. Eng. J. **369**, 1150–1160 (2019)

7. D. Bao, Y. Cui, F. Xu, M. Li, K. Li, X. Zhang, Z. Liu, Y. Zhu, H. Wang, High thermal conductivity of epoxy composites via micro-zone enhanced 3D interconnected nickel skeleton. Ceram. Int. **46**, 27531–27538 (2020)

8. L. Chen, C. Xiao, Y. Tang, X. Zhang, K. Zheng, X. Tian, Preparation and properties of boron nitride nanosheets/cellulose nanofiber shear-oriented films with high thermal conductivity. Ceram. Int. **45**, 12965–12974 (2019)

9. A. Kaźmierczak-Bałata, L. Grządziel, M. Guziewicz, V. Venkatachalapathy, A. Kuznetsov, M. Krzywiecki, Correlations of thermal properties with grain structure, morphology, and defect balance in nanoscale polycrystalline ZnO films. Appl. Surf. Sci. **546**, 149095 (2021)

10. D. Pan, Q. Li, W. Zhang, J. Dong, F. Su, V. Murugadoss, Y. Liu, C. Liu, N. Naik, Z. Guo, Highly thermal conductive epoxy nanocomposites filled with 3D BN/C spatial network prepared by salt template assisted method. Compos. Part B **209**, 108609 (2021)

11. R. Yamamoto, D. Kowalski, R. Zhu, K. Wada, Y. Sato, S. Kitano, C. Zhu, Y. Aoki, H. Habazaki, Fabrication of superhydrophobic copper metal nanowire surfaces with high thermal conductivity. Appl. Surf. Sci. **537**, 147854 (2021)

12. P. Zhang, Q. Li, Y. Xuan, Thermal contact resistance of epoxy composites incorporated with nano-copper particles and the multi-walled carbon nanotubes. Compos. Part A **57**, 1–7 (2014)

13. Y. Hu, G. Du, N. Chen, A novel approach for Al_2O_3/epoxy composites with high strength and thermal conductivity. Compos. Sci. Technol. **124**, 36–43 (2016)

14. J. Gu, Z. Lv, Y. Wu, R. Zhao, L. Tian, Q. Zhang, Enhanced thermal conductivity of SiCp/PS composites by electrospinning–hot press technique. Compos. Part A **79**, 8–13 (2015)

15. B. Nan, K. Wu, W. Chen, Y. Liu, Q. Zhang, M. Lu, A combination of nanodiamond and boron nitride for the preparation of polyvinyl alcohol composite film with high thermal conductivity. Appl. Surf. Sci. **508**, 144797 (2020)

16. L. Li, Y. Qin, H. Wang, M. Li, G. Song, Y. Wu, X. Wei, Z. Ali, J. Yi, S. Song, C. Lin, N. Jiang, J. Yu, Improving thermal conductivity of poly(vinyl alcohol) composites by using functionalized nanodiamond. Compos. Commun. **23**, 100596 (2021)

17. Y. Liu, K. Wua, F. Luo, M. Lu, F. Xiao, X. Du, S. Zhang, L. Liang, M. Lu, Significantly enhanced thermal conductivity in polyvinyl alcohol composites enabled by dopamine modifified graphene nanoplatelets. Compos. Part A **117**, 134–143 (2019)

18. T. Ha, D. Kim, J. Ka, Y. Kim, W. Koh, H. Lim, Y. Yoo, Simultaneous effects of silver-decorated graphite nanoplatelets and anisotropic alignments on improving thermal conductivity of stretchable poly(vinyl alcohol) composite films. Compos. Part A **138**, 106045 (2020)

19. G.M. Aparicioa, R.A. Vargasb, P.R. Buenoc, Protonic conductivity and thermal properties of cross-linked PVA/TiO$_2$ nanocomposite polymer membranes. J. Non-Cryst. Solids **522**, 119520 (2019)

20. D. Fan, X. Lv, J. Feng, S. Zhang, J. Xie, J. Liu, Integrating CoNi nanoparticles encapsulated by few-layer h-BN with excellent thermal conductivity and thermal stability. J. Alloy. Comp. **704**, 701–706 (2017)

21. H. Cheng, K. Zhao, Y. Gong, X. Wang, R. Wang, F. Wang, R. Hu, F. Wang, X. Zhang, J. He, X. Tian, Covalent coupling regulated thermal conductivity of poly(vinyl alcohol)/ boron nitride composite fifilm based on silane molecular structure. Compos. Part A **137**, 106026 (2020)

22. S.K. Biswas, H. Sano, M.I. Shams, H. Yano, Three-dimensional-moldable nanofiber-reinforced transparent composites with a hierarchically self-assembled "Reverse" nacre like architecture. ACS Appl. Mater. Inter. **9**, 30177–30184 (2017)

23. G. Pan, Y. Yao, X. Zeng, J. Sun, J. Hu, R. Sun, J.B. Xu, C.P. Wong, Learning from natural nacre: constructing layered polymer composites with high thermal conductivity. ACS Appl. Mater. Inter. **9**, 33001–33010 (2017)

24. J. Chen, X.Y. Huang, B. Sun, Y.X. Wang, Y.K. Zhu, P.K. Jiang, Vertically aligned and interconnected boron nitride nanosheets for advanced flexible nanocomposite thermal interface materials. ACS Appl. Mater. Inter. **9**, 30909–30917 (2017)

25. J.W. Gu, Z.Y. Lv, Y.L. Wu, Y.Q. Guo, L.D. Tian, H. Qiu, W.Z. Li, Q.Y. Zhang, Dielectric thermally conductive boron nitride/polyimide composites with outstanding thermal stabilities via in-situ polymerization-electrospinning-hot press method. Compos. Part A-Appl. S. **94**, 209–216 (2017)

26. Y. Zhan, Z. Long, X. Wan, C. Zhan, J. Zhang, Y. He, Enhanced dielectric permittivity and thermal conductivity of

hexagonal boron nitride/poly(arylene ether nitrile) composites through magnetic alignment and mussel inspired co-modification. Ceram. Int. **43**, 12109–12119 (2017)

27. K. Kim, H. Ju, J. Kim, Filler orientation of boron nitride composite via external electric field for thermal conductivity enhancement. Ceram. Int. **42**, 8657–8663 (2016)

28. J. Zhang, X. Wang, C. Yu, Q. Li, Z. Li, C. Li, H. Lu, Q. Zhang, J. Zhao, M. Hu, Y. Yao, A facile method to prepare flexible boron nitride/poly(vinyl alcohol) composites with enhanced thermal conductivity. Compos. Sci. Technol. **149**, 41–47 (2017)

29. Z. Gao, Q. Zhao, C. Li, S. Wang, L. Dong, G.H. Hu, Q. Yang, C. Xiong, A novel fluid-filler/polymer composite as high-temperature thermally conductive and electrically insulating material. Compos. Sci. Technol. **150**, 128–134 (2017)

30. G. Lian, C.C. Tuan, L. Li, S. Jiao, Q. Wang, K.S. Moon, D. Cui, C.P. Wong, Vertically aligned and interconnected graphene networks for high thermal conductivity of epoxy composites with ultralow loading. Chem. Mater. **28**, 6096–6104 (2016)

31. J. Hu, Y. Huang, Y. Yao, G. Pan, J. Sun, X. Zeng, R. Sun, J.B. Xu, B. Song, C.P. Wong, Polymer composite with improved thermal conductivity by constructing a hierarchically ordered three-dimensional interconnected network of BN. ACS Appl. Mater. Inter. **9**, 13544–13553 (2017)

32. E.K. Sam, J. Liu, X.M. Lv, Surface Engineering Materials of Superhydrophobic Sponges for Oil/Water Separation: A Review. Ind. Eng. Chem. Res. **60**, 2353–2364 (2021)

33. L. Li, K. Wang, Z. Huang, C. Zhang, T. Liu, Highly ordered graphene architectures by duplicating melamine sponges as a three-dimensional deformation-tolerant electrode. Nano Res. **9**, 2938–2949 (2016)

34. X. Wang, P. Wu, Melamine foam-supported 3D interconnected boron nitride nanosheets network encapsulated in epoxy to achieve significant thermal conductivity

35. N. Wang, G. Yang, H. Wang, C. Yan, R. Sun, C.P. Wong, A universal method for large-yield and high-concentration exfoliation of two-dimensional hexagonal boron nitride nanosheets. Mater. Today **27**, 33–42 (2019)

36. D. Fan, Q. Zhou, X. Lv, J. Jing, Z. Ye, S. Shao, J. Xie, Synthesis, thermal conductivity and anti-oxidation properties of copper nanoparticles encapsulated within few-layer h-BN. Ceram. Int. **44**, 1205–1208 (2018)

37. W. Choi, K. Choi, C. Yu, Ultrafast nanoscale polymer coating on porous 3D structures using microwave irradiation. Adv. Funct. Mater. **28**, 1704877 (2018)

38. H. Fang, X. Zhang, Y. Zhao, S.L. Bai, Dense graphene foam and hexagonal boron nitride filled PDMS composites with high thermal conductivity and breakdown strength. Compos. Sci. Technol. **152**, 243–253 (2017)

39. X. Wang, Q. Weng, X. Wang, X. Li, J. Zhang, F. Liu, X. Jiang, H. Guo, N. Xu, D. Golberg, Y. Bando, Biomass-sirected synthesis of 20 g high-quality boron nitride nanosheets for thermoconductive polymeric composites. ACS Nano **8**, 9081–9088 (2014)

40. O.H. Kwon, T. Ha, D.G. Kim, B.G. Kim, Y.S. Kim, T.J. Shin, W.G. Koh, H.S. Lim, Y. Yoo, Anisotropy-driven high thermal conductivity in stretchable poly(vinyl alcohol)/hexagonal boron nitride nanohybrid films. ACS Appl. Mater. Inter. **10**, 34625–34633 (2018)

41. X. Zeng, Y. Yao, Z. Gong, F. Wang, R. Sun, J. Xu, C.P. Wong, Ice-templated assembly strategy to construct 3D boron nitride nanosheet networks in polymer composites for thermal conductivity improvement. Small **11**, 6205–6213 (2015)